sustainability

MDPI

Article

Spatiotemporal Drought Assessment Based on Gridded Standardized Precipitation Index (SPI) in Vulnerable Agroecosystems

Stavros Sakellariou [1,*], Marios Spiliotopoulos [2], Nikolaos Alpanakis [2], Ioannis Faraslis [1], Pantelis Sidiropoulos [3], Georgios A. Tziatzios [2], George Karoutsos [4], Nicolas R. Dalezios [2] and Nicholas Dercas [5]

[1] Department of Environmental Sciences, University of Thessaly, 41500 Larisa, Greece; faraslis@uth.gr
[2] Laboratory of Hydrology and Aquatic Systems Analysis, Department of Civil Engineering, University of Thessaly, 38221 Volos, Greece; spilioto@uth.gr (M.S.); nalpanakis@uth.gr (N.A.); getziatz@uth.gr (G.A.T.); dalezios.n.r@gmail.com (N.R.D.)
[3] Laboratory of Hydraulic Works and Environmental Management, School of Rural and Surveying Engineering, Aristotle University of Thessaloniki, 54124 Thessaloniki, Greece; pasidirop@topo.auth.gr
[4] General Aviation Applications "3D" S.A., 2 Skiathou Str., 54646 Thessaloniki, Greece; karougeo@3dsa.gr
[5] Department of Natural Resources Management and Agricultural Engineering, Agricultural University of Athens, 11855 Athens, Greece; ndercas1@aua.gr
* Correspondence: stasakel@uth.gr

Abstract: Drought is one of the most critical environmental hazards for the viability and productive development of crops, especially in a climate change environment. To this end, drought assessment is a process of paramount importance to make vulnerable agricultural regions more resilient. The primary aim of this paper is an integrated drought assessment through time and space in one of the most susceptible (in terms of water availability limitations) and agriculturally productive regions in Greece and the Mediterranean, namely, the Thessaly region. Supplementary objectives consist of the determination of the two most extreme years in terms of drought and wetness, so that we may reveal any potential climatological cycles/patterns from 1981 to 2020. Additionally, the methodology includes the annual and seasonal analysis using one of the most widely used drought indices, namely, the Standardized Precipitation Index (SPI), so that consistent measurements are available across a large study area, avoiding the possible scarcity/deficiency of data coming from a sparse land weather network. The innovative element of this paper is the integrated spatiotemporal drought assessment in multiple time scales through the estimation of the SPI making use of remotely sensed data, such as CHIRPS (Climate Hazards Group InfraRed Precipitation with Station data). The outcomes highlight that the study area faced two severe years of drought in 1988 and 1989, which led to moderate and extreme drought conditions, respectively. In contrast, extremely wet conditions were observed in 2002–2003, whereas 2009–2010 experienced moderately wet conditions. The central and western part of the region tends to suffer the most in terms of drought severity, especially at the most extreme years. The validity of the results has been confirmed by the adoption of R^2 where the index is approaching 0.67 despite the large size of the pixels (5×5 km). In this context, the mapping of spatial and seasonal variability across the study area permits more targeted measures (e.g., precision farming) instead of horizontal policies.

Keywords: drought; Standardized Precipitation Index; Climate Hazards Group InfraRed Precipitation with Station data; Thessaly; Greece; desertification

check for updates

Citation: Sakellariou, S.; Spiliotopoulos, M.; Alpanakis, N.; Faraslis, I.; Sidiropoulos, P.; Tziatzios, G.A.; Karoutsos, G.; Dalezios, N.R.; Dercas, N. Spatiotemporal Drought Assessment Based on Gridded Standardized Precipitation Index (SPI) in Vulnerable Agroecosystems. *Sustainability* **2024**, *16*, 1240. https://doi.org/10.3390/su16031240

Academic Editor: Mike Spiliotis

Received: 1 December 2023
Revised: 26 January 2024
Accepted: 27 January 2024
Published: 1 February 2024

1. Introduction

Interannual temperature and precipitation anomalies have been observed on a global scale, a fact that is primarily attributed to human activities, such as the burning of fossil fuels, deforestation, and/or land-use changes. All these activities have been releasing a great amount of greenhouse gases into the atmosphere, affecting the natural environment and human health. Consequently, the projected temperature rise may potentially lead to more frequent and intense heat waves, deteriorating the drought episodes. Drought can be defined as a prolonged period of below-average precipitation, which can lead to reduced amounts of river flow, lower groundwater levels, and as a result, various anomalies in the ecosystems, which can affect agricultural and industry activities [1,2]. Drought events are affecting many regions across the Earth and are increasingly frequent, especially in Europe. Recently, Europe has experienced several severe drought events, especially in southern and southeastern regions. Droughts may have a strong impact on the socioeconomic structure of every society, especially in semi-arid regions that are characterized by vulnerable agriculture, such as the Mediterranean region, which receives a shortage of rainfall and has a scarce water supply [2]. Drought events can be attributed to climate change and/or increased demand for water resources. Due to their significance, it is obvious that more actions are needed to define the main causes of this problem and to ensure that society is prepared for the unexpectedly increasing frequency and severity of those events in the future [3]. However, to mitigate the effects of droughts, governments and local authorities should develop specific drought management plans and more sustainable water use practices [4]. Specifically, in Greece, droughts are a frequent situation [5], and a change in the frequency and severity has also been recorded in recent years [6,7], frequently leading to dangerous wildfires, having serious consequences in many regions of the country [8–12].

Drought severity is usually defined through indices [13]. Drought indices are numerical values based on ground (in situ) and/or remotely sensed data [14–21] and are computed for each specific region. For the computation of each specific index, precipitation values are first needed, enriched with temperature or evapotranspiration values according to data availability [22,23]. Some indices also include soil moisture and crop growth indicators. Drought indices is an important tool for the scientific community and/or the related stakeholders, helping to identify risky areas and inform decision-makers about water resource management practices [24–29]. Drought indices should make a standardized way to evaluate the extent of drought conditions and the related changes over time. Generally, drought indices can have some strong capabilities but also some limitations. For instance, the Standardized Precipitation Index (SPI) uses precipitation data to quantify drought/wet conditions, whereas the Palmer Drought Severity Index (PDSI) combines climatic variables such as temperature and precipitation to make a more comprehensive drought assessment [22].

There are several review articles in the international literature presenting and comparing various drought indices [30–38]. There are also many extensive studies on drought forecasting based on such indices [39–47]. Remote sensing methodologies can also play an important role in the computation of drought indices. This connection has been achieved using vegetation indices (VIs) which have been introduced in the literature using a combination of surface reflectance values between two or more spectral bands related to satellite systems. Among over a hundred Vis, only a small part has been systematically studied [47]. One of the most prevalent remote sensing indices for the assessment of drought—among others—is the Normalized Difference Vegetation Index [48,49]. NDVI or similar indices like Vegetation Condition Index (VCI) derived from satellite systems can provide satisfactory temporal and spatial coverage over the Earth, making the related computations potentially easier and relatively less expensive than conventional ones [46,48,49]. The SPI has been selected to be adopted for the study area because it has already been tested globally with very reliable results [47,50–52]. The SPI is based on a probability distribution function and is a standardized index, and as a result, it can be applied to various climate types all over the world. Numerous research studies investigated drought events using the SPI [52–54]. Previous studies in the region of Thessaly investigated the impact of drought to assess stress on crop yields and to evaluate the effectiveness of drought on crop yield assessment [53,54]. Other studies have used the SPI and other drought indices to investigate the frequency and severity of drought events, as well as to identify the most vulnerable regions to drought, especially in Greece [5,55–58]. More recently, Anagnostopoulou [58], Paparizos et al. [59], Georgoulias et al. [60], and Politi et al. [61] have attempted a future projection using the SPI under different climate conditions, whereas Kourgialas [62] used the SPI for the study of hydrological extremes in the region. The necessity of the current research is dictated by the frequent advent of drought events in the study area which is the largest agricultural region of the country affecting the primary cultivation crops (e.g., cotton; wheat; corn) of Thessaly. The innovative element of this paper is the integrated spatiotemporal drought assessment in multiple time scales through the estimation of the SPI making use of remotely sensed data, such as CHIRPS. Therefore, satellite-derived data from CHIRPS are utilized instead of conventional meteorological data for the computation of the Standardized Precipitation Index (SPI). Consequently, the objectives of this study are: (i) to conduct a spatiotemporal analysis of drought severity using the SPI for the period 1981–2020 in Thessaly, Greece; (ii) to identify both dry and wet periods; (iii) to classify the degree of drought/wetness conditions using a classification scheme for multiple timescales; and (iv) to calculate and classify SPI_{12} for each month from 1981 to 2020.

2. Materials and Methods

2.1. Study Area

Thessaly serves as the study area. Thessaly is situated in the center of Greece's territory (Figure 1). The agriculture of Thessaly is characterized as vulnerable mainly due to restricted water availability. According to [63], Thessaly soil has a mixture of alfisols, inceptisols, endisols, and vertisols. The dominant cultivation crops consist of cotton, corn, and wheat. The region is mainly plain surrounded by the Aegean Sea to the east, Mount Ossa and Olympus to the north, the peninsula of Magnesia to the east, Othrys Mountain to the south, and the Pindus Range to the west. The plains are being traversed by several rivers that are generated from the nearby mountains. Thessaly's western region experiences a continental climate with extremely cold winters and hot summers, with a significant temperature difference between the two seasons. The climate is warm and humid on Thessaly's eastern edge. The region experiences typically extremely hot and dry summers, with July and August's maximum temperatures exceeding 40 °C. Summer months are often dry and sunny, which is a typical case of a Mediterranean environment. The mountainous regions have substantially lower temperatures and more precipitation. Spring and summer thunderstorms are also usual. As a result, agricultural activities in this area are significantly affected by these phenomena.

Figure 1. Study area.

2.2. Precipitation Data

Climate Hazards Group InfraRed Precipitation with Station data (CHIRPS) database [64] is used as the main data source in this study. CHIRPS database contains gridded daily precipitation data estimated from both rain gauge and satellite observations. The combination of those two sources is the comparative benefit of CHIRPS (Climate Hazards Center, 2022). Gridded daily precipitation data at a spatial resolution of 0.05° and 0.25° for the quasi-global coverage of 50° N–50° S from 1981 to the present can be freely downloaded from this dataset [64,65]. Monthly gridded precipitation data for the period 1981–2020 with a spatial resolution of 5 km were finally retrieved and processed through CHIRPS data for this study.

2.3. Methodology

The primary aim of the research constitutes the spatiotemporal analysis of drought severity. Drought severity estimation requires precipitation data. The Standardized Precipitation Index (SPI), which is suitable for identifying both dry and wet periods [21], has been adopted for this study. The SPI has been developed for multiple timescales to quantify drought in different ground layers. Soil moisture is better described by this index in a shorter timeframe (e.g., 3 or 6 months: SPI_3 or SPI_6 for agricultural drought), whereas the groundwater resources deficit requires the estimation of the SPI for longer periods (12–48 months: hydrological drought) [10,66,67]. Having obtained precipitation data for a long period, the maximum likelihood is applied to calculate the coefficients of gamma distribution and eventually to fit a gamma distribution. Next, the cumulative probability is used for the inverse normal function, resulting in the SPI [68,69]. Therefore, the SPI is estimated by a fraction, where the numerator equals the difference between the long-term seasonal mean and the normalized seasonal precipitation, whereas the denominator equals the standard deviation.

The SPI relies on the normalized probability distribution (Figure 2), which is suitable for the comparative assessment of drought/wetness conditions among different areas. The numerical SPI value is retrieved from a given probability distribution function [65,66,69]. Suppose that x is the cumulated monthly precipitation in the selected time scale (1, 3, 6, 12 months), which fits a gamma probability density function g(x) as follows:

$$g(x) = \frac{1}{\beta^{a}\Gamma(a)} x^{\alpha-1} e^{-\frac{x}{\beta}},\ \mathrm{x} > 0 \tag{1a}$$

$$\Gamma(x) = \int_0^\infty x^{a-1} e^{-x} dx \tag{1b}$$

where x is the precipitation sum, g(x) is the gamma function. In the above Equation (1a,b), a and b are the shape and scale parameter, respectively, which can be estimated by the maximum likelihood method [66,68,69] as follows:

$$\alpha = \frac{1+\sqrt{1+\frac{4A}{3}}}{4A},\ \beta = \frac{x}{a} \tag{2a}$$

$$A = \ln(\overline{x}) - \frac{\sum \ln(x)}{n} \tag{2b}$$

where n is the length (months) of the time series. The resulting cumulative probability of precipitation x in the given time scale is expressed as:

$$G(x) = \int_0^x g(x)dx = \frac{1}{\beta^{\alpha}\Gamma(x)} \int_0^x x^{a-1} e^{-x/\beta} dx \tag{3}$$

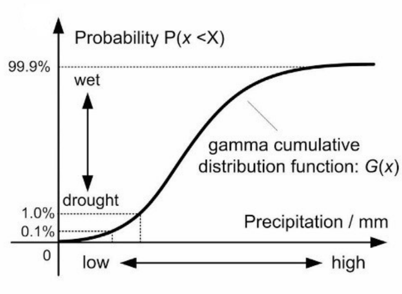

(**a**)

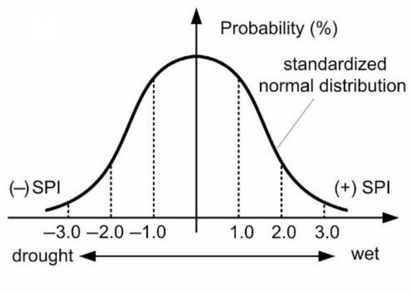

(**b**)

Figure 2. The normalized distribution applied by the SPI: (**a**) fitted gamma distribution for the cumulated monthly precipitation in Equations (3) and (4); (**b**) standardized normal distribution for SPI in Equation (6). Wetness (positive SPI)/dryness (negative SPI) [69].

Let t = x/b and Equation (3) above transforms into an incomplete gamma function:

$$G(x) = \frac{1}{\Gamma(\alpha)} \int_0^x t^{a-1} e^{-t} dt \tag{4}$$

To consider the extreme situation when the cumulated monthly precipitation x = 0, then Equation (4) is modified as H(x):

$$H(x) = q + (1-q)G(x) \tag{5}$$

where q is the probability of x = 0, i.e., the frequency of occurrence of x = 0 in the entire observation series. The SPI is then transformed into the standardized normal distribution function and expressed as:

$$\mathrm{SPI} = \begin{cases} -\left(t - \frac{c_0+c_1+c_2t^2}{1+d_1t+d_2t^2+d_3t^3}\right),\ t = \sqrt{\ln\left(\frac{1}{(H(x))^2}\right)},\ 0 < H(x) \leq\ 0.5 \\ t - \frac{c_0+c_1+c_2t^2}{1+d_1t+d_2t^2+d_3t^3},\ t = \sqrt{\ln\left(\frac{1}{(1-H(x))^2}\right)},\ 0.5 < H(x) < 1 \end{cases} \tag{6}$$

where the constants are c_0 = 2.515517, c_1 = 0.802853, c_2 = 0.010328, d_1 = 1.432788, d_2 = 0.189269, and d_3 = 0.001308.

Based on the above analysis, a classification scheme is used to determine the degree of drought/wetness conditions (Table 1). When the SPI is lower than −1, differentiated degrees of drought are observed. Similarly, when the SPI is higher than 1, differentiated degrees of wet conditions prevail. Finally, SPI_{12} has been calculated for each month through the entire timeframe (1981–2020). Seven classes of the SPI are shown in Table 1 [70,71].

Table 1. SPI classification scheme.

SPI Values	Class	Probability (%)
>2	Extremely wet	2.3
1.5–1.99	Very wet	4.4
1–1.49	Moderately wet	9.2
−0.99–0.99	Normal precipitation	68.2
−1–−1.49	Moderately dry	9.2
−1.5–−1.99	Very dry	4.4
<−2	Extremely dry	2.3

EDO, 2021 (adjusted) [70].

Consequently, SPI_{12} is calculated, which estimates the magnitude of wetness or drought based on precipitation records in the previous 12 months. Precipitation values are adjusted to a “gamma” probability distribution, which is then can be transformed into a normal distribution so that the average SPI values for a specific location must be zero. Severe rainfall deficits which can result in meteorological droughts can be then expressed by SPI values below −1 and lower [72].

Next, the annual meteorological conditions for each hydrological year (from October through September for each calendar year) are estimated. Hence, a new index estimates the average conditions (in terms of normal, wetness, or drought conditions) for each hydrological year. The statistical results were accompanied by a series of thematic maps representing the two driest and wettest conditions in the wider area of Thessaly.

Finally, the annual and monthly spatial distribution of the SPI is mapped by applying the Delaunay triangulation (Voronoi polygons) for each location. The Voronoi polygons [73] have been used to allocate the space of any given region to the closest attribute/station (precipitation measurement: the center of the pixel). This process may provide the necessary tools to enhance the spatial resilience of any given region. For instance, targeted measures against severe drought conditions, before the drought event breaks out, may apply.

3. Results

This section summarizes the results of SPI_{12} evolution in the Thessaly region from 1981 to 2020, highlighting the environmental extremes in terms of drought/wetness. In addition, the spatial variability of this index across the study area for the two driest and wettest hydrological years is mapped. Next, a mapping of intra-annual spatial variability for the driest and wettest hydrological year, enriched with the percentage contribution of extreme conditions, is conducted and presented. These results allow for enhancing the spatial resilience of the Thessaly region, a region with great agricultural significance in Greece.

3.1. Statistical and Geospatial Analysis of Drought/Wetness Severity from 1981 to 2020

The computation of SPI_{12} for the last 30 years in the Thessaly region revealed the environmental extremes throughout the entire time frame. Specifically, the Thessaly region faced two consecutive years of hydrological drought, namely in 1988 and 1989. The annual mean SPI_{12} in 1988–1989 amounts to −1.46, indicating moderate drought conditions, whereas the value for the same index in 1989–1990 amounts to −2.26, indicating extreme drought conditions. Conversely, the annual mean SPI_{12} in 2002–2003 amounts to 2.07 indicating extremely wet conditions, whereas the value for the same index in 2009–2010 amounts to 1.15 indicating moderately wet conditions. Table 2 summarizes the mean annual SPI_{12} evolution in the Thessaly region from 1981 to 2020.

Table 2. Mean annual SPI_{12} evolution in Thessaly region for the hydrological years 1981 to 2020.

Hydrological Year (Oct.–Sep.)	Mean	Hydrological Year (Oct.–Sep.)	Mean
1982	0.404	2002	**2.077**
1983	0.42	2003	0.961
1984	−0.518	2004	−0.144
1985	−0.225	2005	−0.065
1986	−0.283	2006	−0.082
1987	−0.116	2007	−0.538
1988	**−1.462**	2008	0.472
1989	**−2.266**	2009	**1.15**
1990	−0.222	2010	0.631
1991	−0.57	2011	−0.525
1992	−0.936	2012	0.812
1993	−0.346	2013	−0.228
1994	0.617	2014	0.723
1995	0.509	2015	0.178
1996	0.219	2016	−0.419
1997	−0.124	2017	0.432
1998	1.142	2018	0.297
1999	−0.28	2019	−0.009
2000	−1.25	2020	0.236
2001	−0.764		

The driest hydrological year (1989–1990) has affected the entire region horizontally. Based on Figure 3a, it is estimated that almost the entire region of Thessaly is characterized by a high degree of drought (ranging from −2 to −2.96), except for some territories in the western and northern part of the study area, where they face moderate drought conditions (−1.5 < SPI < −1.99). As far as the second driest hydrological year (1988–1989), a differentiated spatial pattern prevails (Figure 3b). Most of the central, western, and northern territory is characterized by moderate drought conditions. Some central and eastern regions face slight drought conditions (−1 < SPI < −1.49), whereas the very eastern region (next to the sea) is characterized by normal conditions ranging from −0.99 to −0.48.

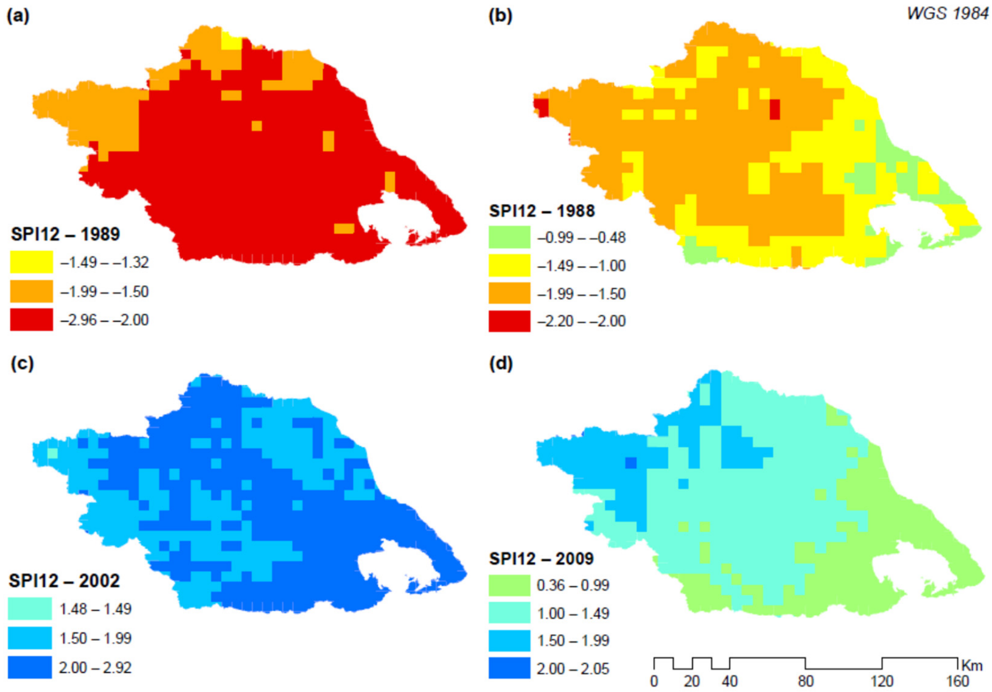

Figure 3. Spatial distribution of SPI_{12} in the (**a**) driest, (**b**) second driest, (**c**) wettest, and (**d**) second wettest hydrological year.

Next, the analysis focused on the two wettest hydrological years. Figure 3c depicts the wettest hydrological year (2002–2003) throughout the time frame, where two primary trends prevail. Very wet conditions (−2 < SPI < −2.92) prevail in many areas of the study domain, specifically through an axis beginning from northwest to southeast. Moderately wet conditions (1.5 < SPI < 1.99) are estimated in the northern and southern territories of the region. In the second wettest hydrological year (2009–2010), there exist some more apparent spatial patterns (Figure 3d). The study area is conceivably divided into three regions with distinct features. The northwestern region is characterized by very wet conditions (1.5 < SPI < 1.99); this region is replaced by the neighboring territory in the center of the study area, which faces moderately wet conditions (1 < SPI < 1.49); the last region is located in the southeast part and is characterized by normal conditions ranging from 0.36 to 0.99.

3.2. Intra-Annual Geospatial Analysis of Drought/Wetness Severity from 1981 to 2020

This section presents the monthly evolution of SPI_{12} across the study domain, as well as the percentage contribution of drought/wetness scales for the driest and wettest hydrological years.

Figure 4 presents the monthly spatial distribution of SPI_{12} in the driest hydrological year. The spatial pattern of drought severity is similar for most of the months. Specifically, it is estimated that almost the entire region is characterized by extreme severity drought (SPI < −2) except a few parts in the northern and northwestern territories of the region which face moderate degrees of drought (−1.5 < SPI < −1.99). This pattern is repeated from

December to September. The only difference lies in October and November. Specifically, in October, most of the region is characterized by moderate drought except for the eastern territory, which faces normal conditions ($-1 < \text{SPI} < 1$). In November, a differentiated pattern is shown, where the southern region is characterized by extreme drought, followed by the central area, which faces less severe drought conditions, whereas some parts in the north and eastern parts are characterized by a low degree of drought.

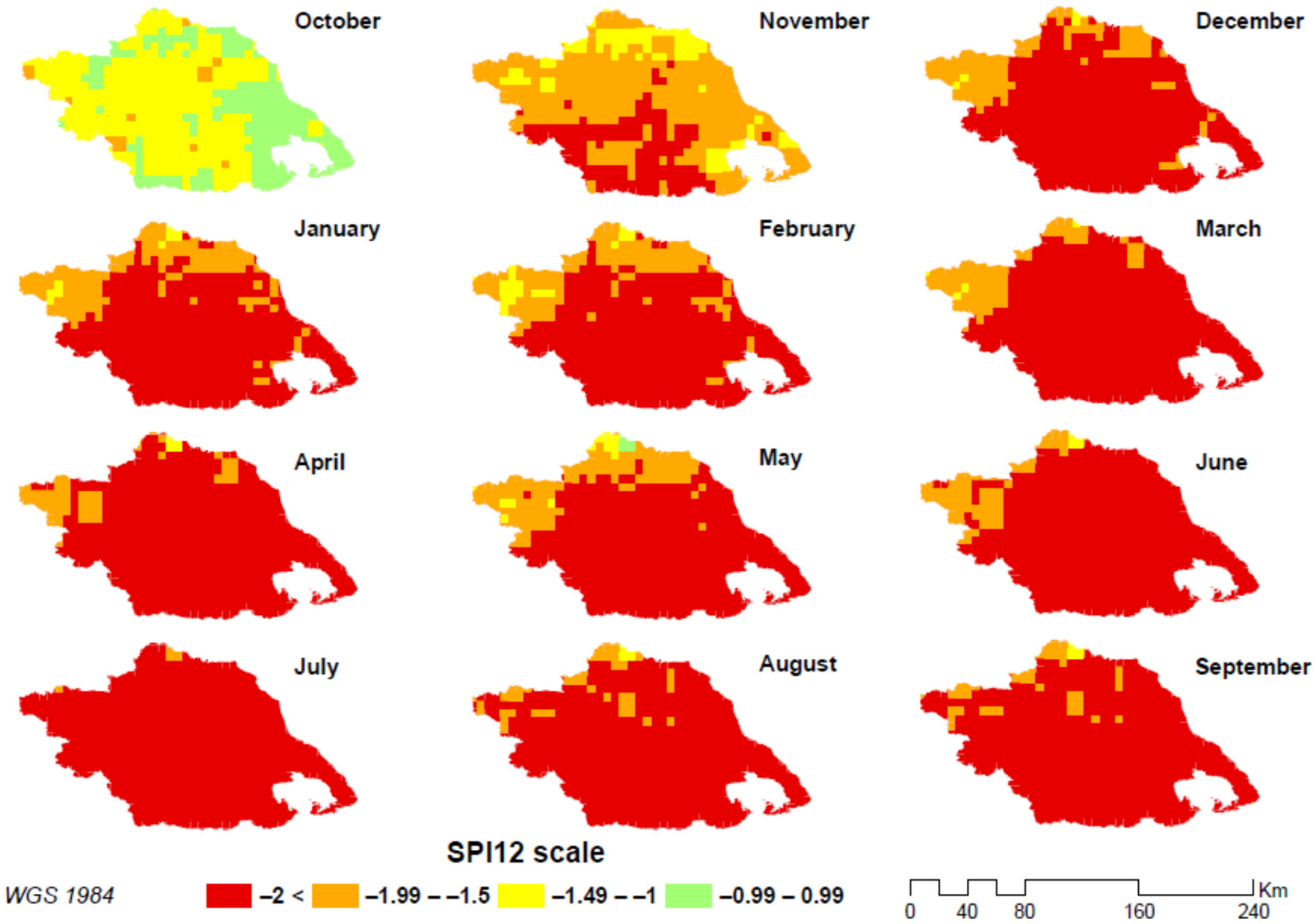

Figure 4. Monthly spatial distribution of SPI_{12} in the driest hydrological year (1989–1990).

Table 3 presents the percentage contribution of each scale of drought as measured by the aggregation of pixels across the entire study area. Table 3 indicates that 71–99% of the study area (in terms of pixels) suffers from extreme drought conditions for all months except October and November. The remaining pixels are primarily characterized by severe drought conditions. October is the least affected month, where 60% of the region is being characterized by moderate drought conditions and 36% by normal conditions. November is a transitional month, when drought conditions are getting worse, representing 60% of severe drought and 25% of extreme drought of the entire territory.

Figure 5 presents the monthly spatial distribution of SPI_{12} in the wettest hydrological year. A very similar pattern is estimated for most of the months, namely from January to August, where almost the entire region is characterized by very wet conditions (SPI > 2). Some diversified spatial patterns are presented in a few months. For instance, the western territory is characterized by normal conditions ($-1 < \text{SPI} < 1$), whereas the eastern territory of the region faces moderately wet conditions ($1 < \text{SPI} < 1.5$) in October and November. In December, an escalating pattern of wetness is observed from west to east. Specifically, the very western territory is characterized by normal conditions, followed by the neighboring area with moderately wet conditions. The subsequent territory is characterized by very wet conditions moving to the east, followed by the very eastern area, which faces extremely wet conditions. Finally, in September, a central territory with moderate wet conditions is encircled by areas that face very wet and extremely wet conditions.

Table 3. Percentage contribution of pixels falling in different categories of drought.

Year	Month	Normal Conditions	Moderate Drought	Severe Drought	Extreme Drought
1989	October	36%	60%	4%	0%
1989	November	0%	15%	60%	25%
1989	December	0%	1%	21%	78%
1990	January	0%	2%	26%	72%
1990	February	0%	4%	25%	71%
1990	March	0%	1%	16%	83%
1990	April	0%	0%	11%	89%
1990	May	1%	2%	23%	74%
1990	June	0%	1%	14%	85%
1990	July	0%	0%	1%	99%
1990	August	0%	1%	9%	90%
1990	September	0%	1%	9%	90%

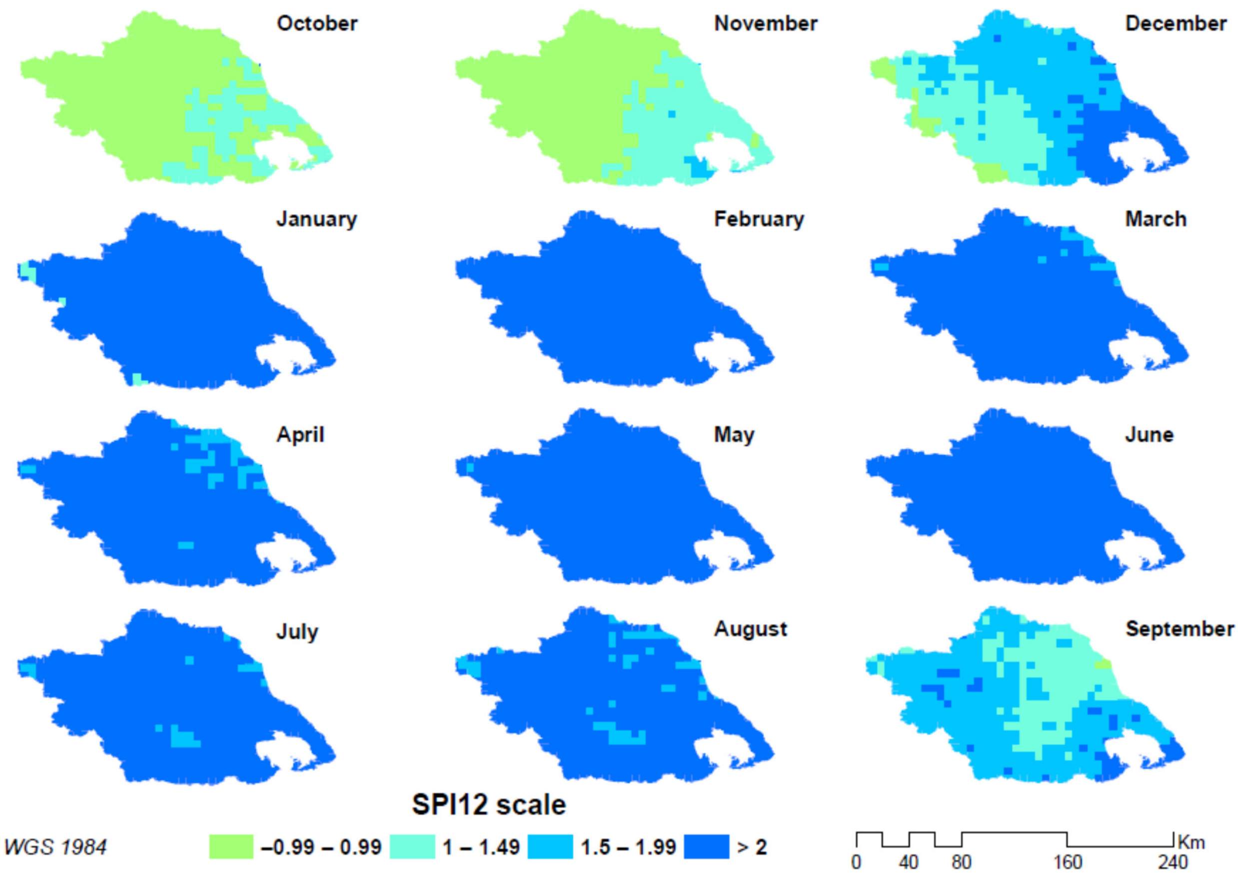

Figure 5. Monthly spatial distribution of SPI_{12} in the wettest hydrological year (2002–2003).

Table 4 summarizes the percentage contribution of each scale of wetness as measured by the aggregation of pixels across the entire study domain. The Table indicates that from January to August, extremely wet conditions prevail in almost the entire study area (from 91 to 100% of the region). Moderate to very wet conditions prevail in December and September, when 27% of the region is characterized by moderately wet conditions, whereas 42% and 61% are characterized by very wet conditions, respectively. Only in October and November, 64–77% of the region is characterized by normal conditions.

Table 4. Percentage contribution of pixels falling in different categories of wetness.

Year	Month	Normal Conditions	Moderate Wet	Very Wet	Extremely Wet
2002	October	77%	22%	1%	0%
2002	November	64%	32%	3%	1%
2002	December	8%	27%	43%	22%
2003	January	0%	0%	2%	98%
2003	February	0%	0%	0%	100%
2003	March	0%	0%	4%	96%
2003	April	0%	0%	8%	92%
2003	May	0%	0%	0%	100%
2003	June	0%	0%	0%	100%
2003	July	0%	0%	4%	96%
2003	August	0%	0%	9%	91%
2003	September	1%	27%	61%	11%

3.3. Validation

This section aims to explore the accuracy of the gridded SPI_{12} index (i.e., from CHIRPS database) as compared to conventional measurements from in situ meteorological stations, where the in situ measurements are considered objectively accurate, since they represent a direct point of quantitative precipitation measurements. A common database was developed consisting of 21 years (1982–2002) of monthly precipitation measurements from eight (8) meteorological stations which are mainly located in the western and central part of Thessaly and the corresponding monthly gridded precipitation data from the CHIRPS database for the pixels above each of the eight stations, respectively. The determination coefficient R^2 is computed from the monthly time series (21 years) of each of the eight stations and the corresponding gridded precipitation pixel values (from the CHIRPS database) above each station, respectively. The formula of R^2 is mathematically expressed as follows [74]:

$$R^2 = 1 - \frac{\sum_i^m (X_i - Y_i)^2}{\sum_i^m (\overline{Y} - Y_i)^2} \tag{7}$$

where X_i is the predicted ith value, Y_i is the actual ith value, and $\overline{Y}$ the mean of the true values

Table 5 presents the coordinates of each station and the computed R^2, which are all above 0.6, with the lowest value being 0.62 in Xalkiades and the greatest value being 0.74 in Kapnikos. These results range within the same order of magnitude as most similar existing comparisons between environmental data. It is also stated that there is a sampling problem since the comparison is attempted between point monthly precipitation values, which are considered objectively accurate, and gridded areal-averaged values (5 × 5 km) of precipitation estimates, which are spatially smoothed values. Based on the above, these results are considered reasonable and acceptable, and thus, the remotely sensed data can sufficiently substitute or complement the conventional data, especially where there is a shortage of meteorological stations across extensive regions.

Table 5. Variance of SPI_{12} index between conventional and remotely sensed data (1982–2002).

Location	X	Y	R^2
Kalampaka	296,882.00	4,396,738.00	0.64
Kapnikos	320,334.96	4,357,401.22	0.74
Karditsomagoyla	320,420.33	4,361,100.99	0.66
Larisa	363,919.00	4,387,859.00	0.65
Morfovouni	305,915.00	4,357,630.00	0.64
Trikala	307,901.00	4,379,795.00	0.66
Xalkiades	363,597.53	4,361,486.00	0.62
Zappeio	366,461.00	4,369,310.00	0.72

4. Discussion

The study mapped the spatial variability of SPI_{12} across the study area for the driest and wettest years, as well as the intra-annual spatial variability for the driest and wettest years, enriched with the percentage contribution of extreme conditions. The mean annual SPI_{12} values showed that there were very few hydrological years with extreme meteorological conditions. Hence, the Thessaly region has experienced extreme environmental conditions over the entire timeframe, including two consecutive years of hydrological drought in 1988–1989 and 1989–1990, and two extremely wet years in 2002–2003 and 2009–2010. The driest year (1989–1990) had a severe impact on the entire region, with almost all parts of the region experiencing high degrees of drought. In this context, Loukas and Vasiliades [75] stated that the hydrological year 1989–1990 was one of the driest years recorded in Thessaly when working with SPI values. Karavitis et al. [76] showed that 1989–1990 was indeed one of the driest years throughout Greece. The same pattern is validated from other similar studies [5,77]. Vasiliades [78] revealed that the hydrological year 1976–1977 was the driest recorded year, whereas the second one was 1989–1990, which was characterized as a severe drought event. Unfortunately, the hydrological year 1976–1977 is not included in the present study, and as a result, the relevant time series is different from the previous ones, which has an impact on the computation of the index, especially when dealing with the specific parameters driven for the estimation of SPI values.

In contrast, the wettest year (2002–2003) showed very wet conditions prevailing in many parts of the study area. This is also validated by Kourtis et al. [77]. A previous study using the Reconnaissance Drought Index (RDI) is also in accordance with the previous assumption [78]. In the wettest hydrological year, the study finds a very similar pattern for most of the months, with almost the entire area characterized by very wet conditions from January to August, with some exceptions with differentiated spatial patterns presented in a few months. In December, the study observes a gradient pattern of wetness from west to east. The study also finds that from January to August, extremely wet conditions prevail in almost the entire study area, and moderate to very wet conditions in December and September, whereas only in October and November, from 64 to 77% of the region is characterized by normal conditions.

Regarding the intra-annual variation, January and February were the driest months recorded during the hydrological year 1989–1990 according to [75]. The present study comes in accordance with this finding (Table 3). Further analysis highlights that the spatial distribution of drought severity in the driest hydrological year is similar for most months, with almost the entire region characterized by extreme drought severity, except for some parts in the northern and northwestern territory which face a moderate degree of drought. However, there is a differentiated pattern in October and November, where most of the region is characterized by moderate drought in October and a differentiated pattern of drought severity in November. The study also revealed that 71–99% of the study area (in terms of pixels) suffers from extreme drought conditions for all months except October and November. Figure 6 illustrates an intra-annual comparison for the hydrological year 1989–1990 between SPI_{12} values derived from the present methodology and conventional values retrieved from [78]. Although the shape of the lines presents a similar behavior, it is obvious that the presented methodology illustrates greater absolute values than the conventional one. This may be explained by the different time series used for the normalization of SPI_{12} values between the two methodologies.

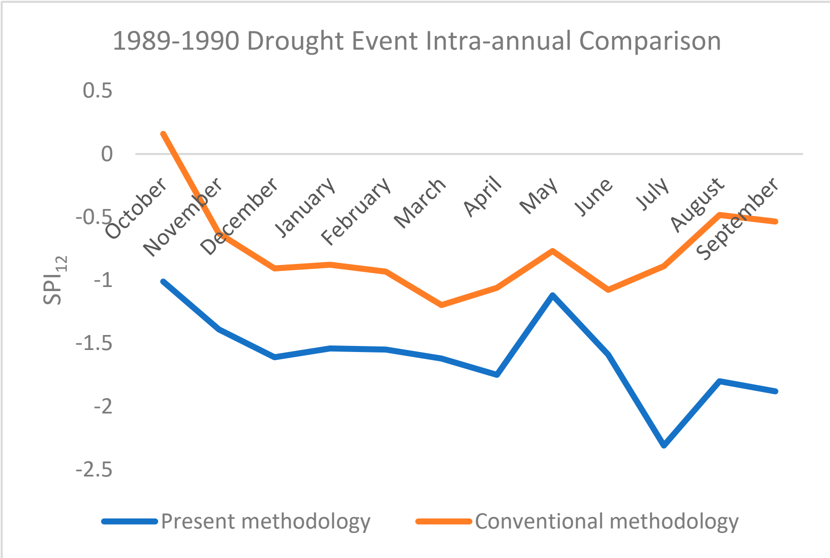

Figure 6. The 1989–1990 SPI_{12} intra-annual comparison between the present methodology and conventional methodology derived from [78].

The analysis revealed differentiated spatial patterns among the regions of the Thessaly area. The central, western, and northern parts of the territory experienced moderate drought conditions, whereas some of the central and eastern regions faced slight drought conditions. The very eastern region, next to the sea, was characterized by normal conditions. In contrast, the northwestern region was characterized by very wet conditions, followed by the neighboring territory in the center of the study area, which faced moderate wet conditions. The last region, located in the southeast, was characterized by normal conditions. Indeed, as stated in [79], Pindos Mountain divides continental Greece into western and eastern regions, and the typical climate of mountainous regions with high annual precipitation and strong gradients of precipitation and temperature is gradually converted to the Mediterranean type. The use of the SPI_{12} index can help to identify extreme conditions and understand the spatial and temporal patterns of these conditions, which can aid in developing strategies to manage the impacts of drought and wetness on the region's agricultural systems [80].

In the same context, a geospatial analysis of future projections of extreme drought incidents could provide a valuable preventative tool for the most affected regions. Politi et al. [61] presented a similar approach to making future projections in Greece using SPI and ERA5 data. The authors have already begun to conduct a preliminary analysis of other Mediterranean regions to enhance climate resilience.

Overall, the study provides a comprehensive analysis of the spatial and temporal patterns of environmental extremes (drought/wetness) across the study domain, based on the SPI_{12} index. The results can help to understand the severity and frequency of drought and wetness events, a fact that is important for rational water resources management and planning, agriculture, and other sectors that may be affected by climate variability. The results of the current analysis can contribute to the enhancement of the spatial resilience of the Thessaly region, an area with high agricultural importance in Greece. Finally, based on the above results, farmers should take advantage of precision agriculture technologies, exploiting, for instance, Internet of things (IoT) devices for the estimation of actual water consumption [81] as well as smart irrigation systems to improve water use efficiency, adopting state-of-the-art wireless communication technologies and sophisticated irrigation control and monitoring systems [82,83]. In the same context, [84] developing sensor cloud-based precision agriculture for water resource optimization reduces the environmental footprint of the agricultural sector and enhances crop productivity. Such technologies should be applied, especially in those areas that are characterized by a high degree of drought as mapped in the above analysis.

5. Conclusions

In this paper, an integrated spatiotemporal drought assessment of the Thessaly region was conducted, taking advantage of the Standardized Precipitation Index (SPI_{12}) for almost 30 years (1981–2020). The index was computed using monthly CHIRPS data as the main input. The results show that the region experienced two consecutive dry hydrological years (1988–1989 and 1989–1990), which can be considered moderately and extremely dry conditions, respectively. Additionally, wet conditions were observed in two cases. The first one was the hydrological year 2002–2003, considered extremely wet, whereas 2009–2010 experienced moderately wet conditions. The spatial variability of the index was mapped for both dry and wet cases, and as a result, a considerable spatial variation was found throughout the region. An intra-annual geospatial analysis was also made, indicating that drought severity was high for most of the months in the driest hydrological year. The same but reverse pattern was almost found for the wettest hydrological year.

These research results were validated by previous studies in the region and can constitute a useful tool for water management practices. Future studies will concentrate on other regions with significant agricultural importance in Greece or in the Mediterranean basin, especially in similar semi-arid climates. Additionally, the authors have already started to use future projections of extreme incidents in order to estimate drought forecasts and contribute to a more feasible water management policy.

Author Contributions: Conceptualization, S.S., N.A., G.A.T. and I.F.; methodology, S.S., N.A. and I.F.; software, S.S., N.A. and G.A.T.; validation, M.S., N.A., S.S. and P.S.; formal analysis, P.S.; investigation, G.K.; resources, G.K.; data curation, G.K.; writing—original draft preparation, M.S. and S.S.; writing—review and editing, M.S.; visualization, N.R.D. and N.D.; supervision, N.R.D. and N.D.; project administration, S.S. and N.R.D.; funding acquisition, N.R.D. and N.D. All authors have read and agreed to the published version of the manuscript.

Funding: This research was co-financed by the European Regional Development Fund of the European Union and Greek national funds through the Operational Program Competitiveness, Entrepreneurship, and Innovation under the call RESEARCH-CREATE-INNOVATE (project code: T2EDK-05354 -EXTREMES). This research is also partly funded by the European PRIMA 2019 HubIS (Hub for Irrigation Systems) project (2020–2024) and the national "Clima Water" project (2023–2025) under the program Metro-16 of the Department of Agricultural and Food Development.

Data Availability Statement: The data presented in this study are available on request from the corresponding author. The data are not publicly available due to privacy restrictions.

Acknowledgments: The authors acknowledge the Climate Hazards Center and USGS Climate for the provided data.

Conflicts of Interest: Author George Karoutsos was employed by the company General Aviation Applications "3D" S.A. The remaining authors declare that the research was conducted in the absence of any commercial or financial relationships that could be construed as a potential conflict of interest.

References

1. Sheffield, J.; Wood, E.F. Projected Changes in Drought Occurrence under Future Global Warming from Multi-Model, Multi-Scenario, IPCC AR4 Simulations. *Clim. Dyn.* **2008**, *31*, 79–105. [CrossRef]
2. Dai, A. Drought under Global Warming: A Review. *Wiley Interdiscip. Rev. Clim. Change* **2011**, *2*, 45–65. [CrossRef]
3. IPCC. *Managing the Risks of Extreme Events and Disasters to Advance Climate Change Adaptation. A Special Report of Working Groups I and II of the Intergovernmental Panel on Climate Change*; Field, C.B., Barros, V., Stocker, T.F., Qin, D., Dokken, D.J., Ebi, K.L., Mastrandrea, M.D., Mach, K.J., Plattner, G.-K., Allen, S.K., et al., Eds.; Cambridge University Press: Cambridge, UK; New York, NY, USA, 2012; 582p.
4. Makhlouf, B.S.I.; Khalil, S.R.A.E.; Saudy, H.S. Efficacy of humic acids and chitosan for enhancing yield and sugar quality of sugar beet under moderate and severe drought. *J. Soil Sci. Plant Nutr.* **2022**, *22*, 1676–1691. [CrossRef]
5. Dalezios, N.R.; Loukas, A.; Vasiliades, L.; Liakopoulos, E. Severity-Duration-Frequency Analysis of Droughts and Wet Periods in Greece. *Hydrol. Sci. J.* **2000**, *45*, 751–769. [CrossRef]

6. Hoerling, M.P.; Quan, X.W.; Eischeid, J.K.; Perlwitz, J. On the Increased Frequency of Mediterranean Drought. *J. Climate* **2012**, *25*, 2146–2161. [CrossRef]
7. Williams, A.P.; Allen, C.D.; Macalady, A.K.; Griffin, D.; Woodhouse, C.A.; Meko, D.M.; Swetnam, T.W. Temperature as a Potent Driver of Regional Forest Drought Stress and Tree Mortality. *Nat. Clim. Chang.* **2013**, *3*, 292–297. [CrossRef]
8. Sakellariou, S.; Cabral, P.; Caetano, M.; Pla, F.; Painho, M.; Christopoulou, O.; Sfougaris, A.; Dalezios, N.; Vasilakos, C. Remotely sensed data fusion for spatiotemporal geostatistical analysis of forest fire hazard. *Sensors* **2020**, *20*, 5014. [CrossRef] [PubMed]
9. Sakellariou, S.; Sfougaris, A.; Christopoulou, O.; Tampekis, S. Integrated wildfire risk assessment of natural and anthropogenic ecosystems based on simulation modeling and remotely sensed data fusion. *Int. J. Disaster Risk Reduct.* **2022**, *78*, 103129. [CrossRef]
10. Anagnostopoulou, C. A Contribution to the Drought Analysis in Greece. Ph.D. Thesis, Aristotle University of Thessaloniki, Thessaloniki, Greece, 2003.
11. Caloiero, T.; Veltri, S.; Caloiero, P.; Frustaci, F. Drought Analysis in Europe and in the Mediterranean Basin Using the Standardized Precipitation Index. *Water* **2018**, *10*, 1043. [CrossRef]
12. Pietrapertosa, F.; Olazabal, M.; Simoes, S.; Salvia, M.; Fokaides, P.; Ioannou, B.; Viguié, V.; Spyridaki, N.A.; De Gregorio Hurtado, S.; Geneletti, D.; et al. Adaptation to climate change in cities of Mediterranean Europe. *Cities* **2023**, *140*, 104452. [CrossRef]
13. Saudy, H.S.; El–Samad, G.A.A.; El–Temsah, M.E.; El–Gabry, Y.A.E.G. Effect of iron, zinc, and manganese nano-form mixture on the micronutrient recovery efficiency and seed yield response index of sesame genotypes. *J. Soil Sci. Plant Nutr.* **2022**, *22*, 732–742. [CrossRef]
14. Gao, B.C. NDWI–A normalized difference water index for remote sensing of vegetation liquid water from space. *Remote Sens. Environ.* **1996**, *58*, 257–266. [CrossRef]
15. Svoboda, M.; LeComte, D.; Hayes, M.; Heim, R.; Gleason, K.; Angel, J.; Rippey, B.; Tinker, R.; Palecki, M.; Stooksbury, D.; et al. The Drought Monitor. *Bull. AMS* **2002**, *83*, 1181–1190. [CrossRef]
16. González, J.; Valdés, J. New drought frequency index: Definition and comparative performance analysis. *Water Resour. Res.* **2006**, *42*, W11421. [CrossRef]
17. Brown, J.F.; Wardlow, B.D.; Tadesse, T.; Hayes, J.J.; Reed, B.C. The Vegetation Drought Response Index (VegDri): An integrated approach for monitoring drought stress in vegetation. *GIScience Remote Sens.* **2008**, *45*, 16–46. [CrossRef]
18. Wilhite, D.A. The role of disaster preparedness in national planning with specific reference to droughts. In *Natural Disasters and Extreme Events in Agriculture*; Sivakumar, M.V.K., Motha, R.P., Das, H.P., Eds.; Springer: Berlin/Heidelberg, Germany, 2005; pp. 23–37.
19. Noguera, I.; Domínguez-Castro, F.; Vicente-Serrano, S.M. Characteristics and trends of flash droughts in Spain, 1961–2018. *Ann. N. Y. Acad. Sci.* **2020**, *1472*, 155–172. [CrossRef] [PubMed]
20. Frischen, J.; Meza, I.; Rupp, D.; Wietler, K.; Hagenlocher, M. Drought Risk to Agricultural Systems in Zimbabwe: A Spatial Analysis of Hazard, Exposure, and Vulnerability. *Sustainability* **2020**, *12*, 752. [CrossRef]
21. Mühlbauer, S.; Costa, A.C. A spatiotemporal analysis of droughts and the influence of North Atlantic Oscillation in the Iberian Peninsula based on MODIS imagery. *Theor. Appl. Clim.* **2015**, *124*, 703–721. [CrossRef]
22. Vicente-Serrano, S.M.; Beguería, S.; López-Moreno, J.I. A multiscalar drought index sensitive to global warming: The standardized precipitation evapotranspiration index. *J. Clim.* **2010**, *23*, 1696–1718. [CrossRef]
23. Tsakiris, G.; Vangelis, H. Establishing a Drought Index Incorporating Evapotraspiration. *Eur. Water* **2005**, *9*, 3–11.
24. Bannari, A.; Morin, D.; Bonn, F.; Huete, A.R. A review of vegetation indices. *Remote Sens. Rev.* **1995**, *13*, 95–120. [CrossRef]
25. Nastos, P.T.; Dalezios, N.R.; Faraslis, I.N.; Mitrakopoulos, K.; Blanta, A.; Spiliotopoulos, M.; Sakellariou, S.; Sidiropoulos, P.; Tarquis, A.M. Risk Management Framework of Environmental Hazards and Extremes in Mediterranean Ecosystems. *Nat. Hazards Earth Syst. Sci.* **2021**, *21*, 1935–1954. [CrossRef]
26. WMO. *World Meteorological Organization: Standardized Precipitation Index. User Guide*; WMO: Geneva, Switzerland, 2012.
27. Dalezios, N.R.; Blanta, A.; Spyropoulos, N.V.; Tarquis, A.M. Risk Identification of Agricultural Drought in Sustainable Agroecosystems. *Nat. Hazards Earth Syst. Sci.* **2014**, *14*, 2435–2448. [CrossRef]
28. Elvidge, C.D.; Chen, Z. Comparison of broad-band and narrow-band red and near-infrared vegetation indices. *Remote Sens. Environ.* **1995**, *54*, 38–48. [CrossRef]
29. Xue, J.; Su, B. Significant remote sensing vegetation indices: A review of developments and applications. *J. Sens.* **2017**, *2017*, 1353691. [CrossRef]
30. Kchouk, S.; Melsen, L.A.; Walker, D.W.; Van Oel, P.R. A Geography of Drought Indices: Mismatch between Indicators of Drought and Its Impacts on Water and Food Securities. *Nat. Hazards Earth Syst. Sci.* **2022**, *22*, 323–344. [CrossRef]
31. Zargar, A.; Sadiq, R.; Naser, B.; Khan, F.I. A Review of Drought Indices. *Environ. Rev.* **2011**, *19*, 333–349. [CrossRef]
32. Mishra, A.K.; Singh, V.P. A Review of Drought Concepts. *J. Hydrol.* **2010**, *391*, 202–216. [CrossRef]
33. McVicar, T.R.; Jupp, D.L.B. The Current and Potential Operational Uses of Remote Sensing to Aid Decisions on Drought Exceptional Circumstances in Australia: A Review. *Agric. Syst.* **1998**, *57*, 399–468. [CrossRef]
34. Heim, R.R., Jr. A Review of Twentieth-Century Drought Indices Used in the United States. *Bull. Am. Meteorol. Soc.* **2002**, *83*, 1149–1165. [CrossRef]
35. Keyantash, J.; Dracup, J.A. The Quantification of Drought: An Evaluation of Drought Indices. *Bull. Am. Meteorol. Soc.* **2002**, *83*, 1167–1180. [CrossRef]

36. Niemeyer, S. New drought indices. *Options Méditerranéennes. Série A Séminaires Méditerranéens* **2008**, *80*, 267–274.
37. Sivakumar, M.V.K.; Motha, R.P.; Wilhite, D.A.; Wood, D.A. (Eds.) *Agricultural Drought Indices—Proceedings of an Expert Meeting: 2–4 June, 2010, Murcia, Spain*; WMO: Geneva, Switzerland, 2011; 219p.
38. Piri, J.; Abdolahipour, M.; Keshtegar, B. Advanced Machine Learning Model for Prediction of Drought Indices using Hybrid SVR-RSM. *Water Resour. Manag.* **2022**, *37*, 683–712. [CrossRef]
39. Ojeda, M.G.-V.; Romero-Jiménez, E.; Rosa-Cánovas, J.J.; Yeste, P.; Castro-Díez, Y.; Esteban-Parra, M.J.; Vicente-Serrano, S.M.; Gámiz-Fortis, S.R. Assessing Future Drought Conditions over the Iberian Peninsula: The Impact of Using Different Periods to Compute the SPEI. *Atmosphere* **2021**, *12*, 980. [CrossRef]
40. Arnone, E.; Cucchi, M.; Gesso, S.D.; Petitta, M.; Calmanti, S. Droughts Prediction: A Methodology Based on Climate Seasonal Forecasts. *Water Resour. Manag.* **2020**, *34*, 4313–4328. [CrossRef]
41. Lai, P.; Zhang, M.; Ge, Z.; Hao, B.; Song, Z.; Huang, J.; Ma, M.; Yang, H.; Han, X. Responses of Seasonal Indicators to Extreme Droughts in Southwest China. *Remote Sens.* **2020**, *12*, 818. [CrossRef]
42. del Pilar Jiménez-Donaire, M.; Tarquis, A.; Giráldez, J.V. Evaluation of a combined drought indicator and its predictive potential for agricultural droughts in Southern Spain. *Nat. Hazards Earth Syst. Sci. Discuss* **2019**, *20*, 21–33. [CrossRef]
43. Habibi, B.; Meddi, M.; Torfs, P.J.; Remaoun, M.; Van Lanen, H.A. Characterisation and prediction of meteorological drought using stochastic models in the semi-arid Chéliff–Zahrez basin (Algeria). *J. Hydrol. Reg. Stud.* **2018**, *16*, 15–31. [CrossRef]
44. Tian, M.; Wang, P.; Khan, J. Drought Forecasting with Vegetation Temperature Condition Index Using ARIMA Models in the Guanzhong Plain. *Remote Sens.* **2016**, *8*, 690. [CrossRef]
45. Das, P.K.; Dutta, D.; Sharma, J.R.; Dadhwal, V.K. Trends and behaviour of meteorological drought (1901–2008) over Indian region using standardized precipitation–evapotranspiration index. *Int. J. Climatol.* **2015**, *36*, 909–916. [CrossRef]
46. AghaKouchak, A.; Farahmand, A.; Melton, F.S.; Teixeira, J.; Anderson, M.C.; Wardlow, B.D.; Hain, C.R. Remote sensing of drought: Progress, challenges, and opportunities. *Rev. Geophys.* **2015**, *53*, 452–480. [CrossRef]
47. Spiliotopoulos, M.; Loukas, A. Hybrid Methodology for the Estimation of Crop Coefficients Based on Satellite Imagery and Ground-Based Measurements. *Water* **2019**, *11*, 1364. [CrossRef]
48. Domenikiotis, C.; Spiliotopoulos, M.; Tsiros, E.; Dalezios, N.R. Early cotton production assessment in Greece based on the combination of the drought vegetation condition index (VCI) and Bhalme and Mooley Drought Index (BMDI). *Int. J. Remote Sens.* **2004**, *25*, 5373–5388. [CrossRef]
49. Domenikiotis, C.; Spiliotopoulus, M.; Tsiros, E.; Dalezios, N.R. Early cotton yield assessment by the use of the NOAA/AVHRR derived vegetation condition index (VCI) in Greece. *Int. J. Remote Sens.* **2004**, *25*, 2807–2819. [CrossRef]
50. McKee, T.B.; Doesken, N.J.; Kleist, J. The relationship of drought frequency and duration to time scales. In Proceedings of the 8th Conference on Applied Climatology, Anaheim, CA, USA, 17–22 January 1993; American Meteorological Society: Boston, MA, USA, 1993; pp. 179–184.
51. Guttman, N.B. On the sensitivity of sample L moments to sample size. *J. Clim.* **1994**, *7*, 1026–1029. [CrossRef]
52. Hayes, M.J.; Svoboda, M.D. Monitoring the 1996 drought using the standardized precipitation index. *Bull. Am. Meteorol. Soc.* **1999**, *80*, 429–438. [CrossRef]
53. Merabti, A.; Martins, D.S.; Meddi, M.; Pereira, L.S. Spatial and time variability of drought based on SPI and RDI with various time scales. *Water Resour. Manag.* **2018**, *32*, 1087–1100. [CrossRef]
54. Merabti, A.; Darouich, H.; Paredes, P.; Meddi, M.; Pereira, L.S. Assessing Spatial Variability and Trends of Droughts in Eastern Algeria Using SPI, RDI, PDSI, and MedPDSI—A Novel Drought Index Using the FAO56 Evapotranspiration Method. *Water* **2023**, *15*, 626. [CrossRef]
55. Stathi, E.; Kastridis, A.; Myronidis, D. Analysis of Hydrometeorological Characteristics and Water Demand in Semi-Arid Mediterranean Catchments under Water Deficit Conditions. *Climate* **2023**, *11*, 137. [CrossRef]
56. Tsakiris, G.; Vangelis, H. Towards a Drought Watch System Based on Spatial SPI. *Water Resour. Manag.* **2004**, *18*, 1–12. [CrossRef]
57. Livada, I.; Assimakopoulos, V.D. Spatial and Temporal Analysis of Drought in Greece Using the Standardized Precipitation Index (SPI). *Appl. Clim.* **2007**, *89*, 143–153. [CrossRef]
58. Anagnostopoulou, C. Future Drought Projection for the Greek Region. *Bull. Geol. Soc. Greece* **2017**, *50*, 1038. [CrossRef]
59. Paparrizos, S.; Maris, F.; Weiler, M.; Matzarakis, A. Analysis and Mapping of Present and Future Drought Conditions over Greek Areas with Different Climate Conditions. *Appl. Clim.* **2018**, *131*, 259–270. [CrossRef]
60. Georgoulias, A.K.; Akritidis, D.; Kalisoras, A.; Kapsomenakis, J.; Melas, D.; Zerefos, C.S.; Zanis, P. Climate Change Projections for Greece in the 21st Century from High-Resolution EURO-CORDEX RCM Simulations. *Atmos. Res.* **2022**, *271*, 106049. [CrossRef]
61. Politi, N.; Vlachogiannis, D.; Sfetsos, A.; Nastos, P.T.; Dalezios, N.R. High Resolution Future Projections of Drought Characteristics in Greece Based on SPI and SPEI Indices. *Atmosphere* **2022**, *13*, 1468. [CrossRef]
62. Kourgialas, N. Hydroclimatic impact on mediterranean tree crops area–Mapping hydrological extremes (drought/flood) prone parcels. *J. Hydrol.* **2021**, *596*, 125684. [CrossRef]
63. Golia, E.E.; Diakoloukas, V. Soil Parameters Affecting the Levels of Potentially Harmful Metals in Thessaly Area, Greece: A Robust Quadratic Regression Approach of Soil Pollution Prediction. *Environ. Sci. Pollut. Res.* **2022**, *29*, 29544–29561. [CrossRef] [PubMed]
64. Climate Hazards Center. CHIRPS: Rainfall Estimates from Rain Gauge and Satellite Observations. 2022. Available online: https://www.chc.ucsb.edu/data/chirps (accessed on 28 September 2022).

65. Duan, Z.; Liu, J.; Tuo, Y.; Chiogna, G.; Disse, M. Evaluation of Eight High Spatial Resolution Gridded Precipitation Products in Adige Basin (Italy) at Multiple Temporal and Spatial Scales. *Sci. Total Environ.* **2016**, *573*, 1536–1553. [CrossRef]
66. Qin, Y.; Yang, D.; Lei, H.; Xu, K.; Xu, X. Comparative Analysis of Drought Based on Precipitation and Soil Moisture Indices in Haihe Basin of North China during the Period of 1960–2010. *J. Hydrol.* **2015**, *526*, 55–67. [CrossRef]
67. Steinemann, A. Drought indicators and triggers: A stochastic approach to evaluation. *JAWRA J. Am. Water Resour. Assoc.* **2003**, *39*, 1217–1233. [CrossRef]
68. Guttman, N.B. Accepting the Standardized Precipitation Index: A Calculation Algorithm 1. *JAWRA J. Am. Water Resour. Assoc.* **1999**, *35*, 311–322. [CrossRef]
69. Sidiropoulos, P.; Dalezios, N.R.; Loukas, A.; Mylopoulos, N.; Spiliotopoulos, M.; Faraslis, I.N.; Alpanakis, N.; Sakellariou, S. Quantitative Classification of Desertification Severity for Degraded Aquifer Based on Remotely Sensed Drought Assessment. *Hydrology* **2021**, *8*, 47. [CrossRef]
70. EDO. European Drought Observatory. 2021. Available online: https://edo.jrc.ec.europa.eu/documents/factsheets/factsheet_spi.pdf (accessed on 30 June 2021).
71. Ayub, M.; Ashraf, M.Y.; Kausar, A.; Saleem, S.; Anwar, S.; Altay, V.; Ahmad, S.; Ali, S.; Ahmad, R.; Ahmad, R.; et al. Growth and Physio–Biochemical Responses of Maize (*Zea mays* L.) to Drought and Heat Stresses. *Plant Biosyst.* **2021**, *155*, 535–542. [CrossRef]
72. Loukas, A.; Vasiliades, L.; Tzabiras, J. Evaluation of climate change on drought impulses in Thessaly, Greece. *Eur. Water* **2007**, *17*, 17–28. Available online: https://www.ewra.net/ew/pdf/EW_2007_17-18_02.pdf (accessed on 20 February 2023).
73. Aurenhammer, F.; Klein, R.; Lee, D.T. *Voronoi Diagrams and Delaunay Triangulations*; World Scientific Publishing Company: Singapore, 2013; ISBN 978-981-4449-55-5.
74. Chicco, D.; Warrens, M.J.; Jurman, G. The coefficient of determination R-squared is more informative than SMAPE, MAE, MAPE, MSE and RMSE in regression analysis evaluation. *PeerJ Comput. Sci.* **2021**, *7*, e623. [CrossRef]
75. Loukas, A.; Vasiliades, L. Probabilistic analysis of drought spatiotemporal characteristics in Thessaly Region, Greece. *Nat. Hazards Earth Syst. Sci.* **2004**, *4*, 719–731. [CrossRef]
76. Karavitis, C.A.; Alexandris, S.; Tsesmelis, D.E.; Athanasopoulos, G. Application of the Standardized Precipitation Index (SPI) in Greece. *Water* **2011**, *3*, 787–805. [CrossRef]
77. Kourtis, I.M.; Vangelis, H.; Tigkas, D.; Mamara, A.; Nalbantis, I.; Tsakiris, G.; Tsihrintzis, V.A. Drought Assessment in Greece Using SPI and ERA5 Climate Reanalysis Data. *Sustainability* **2023**, *15*, 15999. [CrossRef]
78. Vasiliades, L. Drought Spatiotemporal Analysis, Modelling and Forecasting in Pinios River Basin of Thessaly, Greece. Ph.D. Thesis, University of Thessaly, Volos, Greece, 2010. Available online: http://hdl.handle.net/10442/hedi/22285 (accessed on 1 November 2023).
79. Blanta, A.; and Spyropoulos, N.V. Assessment of remotely sensed drought features in vulnerable agriculture. *Nat. Hazards Earth Syst. Sci.* **2012**, *12*, 3139–3150. [CrossRef]
80. Logar, I.; van den Bergh, J.C.J.M. Methods to Assess Costs of Drought Damages and Policies for Drought Mitigation and Adaptation: Review and Recommendations. *Water Resour. Manage.* **2013**, *27*, 1707–1720. [CrossRef]
81. Pincheira, M.; Vecchio, M.; Giaffreda, R.; Kanhere, S.S. Cost-effective IoT devices as trustworthy data sources for a blockchain-based water management system in precision agriculture. *Comput. Electron. Agric.* **2021**, *180*, 105889. [CrossRef]
82. Bwambale, E.; Abagale, F.K.; Anornu, G.K. Smart irrigation monitoring and control strategies for improving water use efficiency in precision agriculture: A review. *Agric. Water Manag.* **2022**, *260*, 107324. [CrossRef]
83. Kamienski, C.; Soininen, J.P.; Taumberger, M.; Dantas, R.; Toscano, A.; Salmon Cinotti, T.; Filev Maia, R.; Torre Neto, A. Smart water management platform: IoT-based precision irrigation for agriculture. *Sensors* **2019**, *19*, 276. [CrossRef] [PubMed]
84. Jayalakshmi, M.; Gomathi, V. Sensor-cloud based precision agriculture approach for intelligent water management. *Int. J. Plant Prod.* **2020**, *14*, 177–186. [CrossRef]